Separation Science and Technology
Publication details, including instructions for authors and subscription information:
http://www.informaworld.com/smpp/title~content=t713708471

The Enrichment of the Heavier of Two Gaseous Isotopes by Enhanced Diffusion (example H^2_2/H^1_2)

Marc J. Jaeger[a]
[a] DEPARTMENT OF PHYSIOLOGY COLLEGE OF MEDICINE, UNIVERSITY OF FLORIDA, GAINESVILLE, FLORIDA

To cite this Article Jaeger, Marc J.(1996) 'The Enrichment of the Heavier of Two Gaseous Isotopes by Enhanced Diffusion (example H^2_2/H^1_2)', Separation Science and Technology, 31: 6, 811 — 827
To link to this Article: DOI: 10.1080/01496399608001326
URL: http://dx.doi.org/10.1080/01496399608001326

SEPARATION SCIENCE AND TECHNOLOGY, 31(6), pp. 811–827, 1996

The Enrichment of the Heavier of Two Gaseous Isotopes by Enhanced Diffusion (example H_2^2/H_2^1)

MARC J. JAEGER
DEPARTMENT OF PHYSIOLOGY
COLLEGE OF MEDICINE
UNIVERSITY OF FLORIDA
P.O. BOX 100274, GAINESVILLE, FLORIDA 32610
Telephone: (904) 392-4483

ABSTRACT

Gaseous isotopes may be separated by enhanced diffusion in oscillatory flow. This paper evaluates the application of this method to the enrichment of deuterium. The oscillations of the carrier raise the diffusional flux without changing the diffusional character of the transport. The process has been well studied and is derived from primary principles. It follows Fick's law. Experimental work shows excellent agreement with the theory. The maximal increase of diffusional flux of H_2^2 in water vapor as the carrier by the oscillations reaches 1200 times. The process is tuned for optimal separation from H_2^1. Some modifications of the standard diffusion setup were introduced: The separation ratio was raised 50 times by having the diffusion take place against a low velocity, constant, upstream current of the carrier; the yield was raised 60-fold by concentrating the feed within the reservoir at the high concentration end of the diffusing path. These combined modifications improve the cost effectiveness of the system by several orders. The method may be further improved. It is versatile in that the yield and the separation ratio can be freely chosen over a large range by adjusting the operating conditions.

INTRODUCTION

A number of papers have been published in the past 40 years on diffusion (dispersion) in a moving fluid. The initial work goes back to Taylor who studied dispersion in steady flow, either laminar or turbulent (1). Enhanced diffusion has also been studied in reciprocating, i.e., oscillating flows (2–4). The advantage of this second approach is that a steady-state

mass transfer can be established between two boundaries. The oscillations result in an appreciable enhancement of mass transfer without altering its diffusional character: the enhancement reaches four orders of magnitude in gases; in liquids it exceeds six orders. The enhancement is all the greater the larger the molecular size. This feature is the basis of our attempt to use this mechanism for separation (5).

The diffusion process is greatly altered when it takes place in moving fluid, especially if the fluid undergoes severe shear stress with large velocity gradients. Molecules may diffuse from a region of low velocity to a region of high velocity and reverse. If they have different sizes, they follow different pathways. The result is a mass transfer which shares characteristics with convective transport and with diffusion: the rate of transport may approach that of convection, yet molecules of different size are transported at different rates. Fick's diffusion equation applies. In the following we present a model of a separation process for hydrogen isotopes. Experiments support the theory which is summarized for clarity in an Appendix.

A glossary of symbols is given.

The theory explains how reciprocating motion results in a periodic return of local concentrations along the diffusing path to the same values. Thus, an integration with respect to time and space can be achieved; this integration links sites along the diffusing path that show the same periodicity. As a result, one can treat diffusion in oscillating flow formally as if it were a simple diffusion process even though the actual time-periodic concentrations and mass transfers are much more involved than in simple diffusion. An effective diffusion coefficient D_{eff} replaces the molecular coefficient D_{m} in the newly formulated Fick equation. D_{eff} varies with pipe geometry, fluid mechanics, and gas properties, and it is defined as (6)

$$D_{\text{eff}} = \lambda\omega\Delta x^2 \tag{1}$$

where λ is a nondimensional coefficient
ω is the angular velocity in radians
Δx is the average oscillation amplitude in centimeters

λ depends on pipe radius a, on ω, on the molecular diffusion coefficient D_{m} of the diffusing species, and on the kinematic viscosity of the carrier. Under optimal conditions it reaches a maximum of about 0.01; such conditions exist when the time needed for radial diffusion is close to the time allotted to diffusion by the reversal of the flow (see Appendix). Table 1 illustrates how λ varies as a function of oscillation frequency; the table uses two isotopes of H_2 as examples. It is seen that the frequency f has a strong effect on λ which reaches peaks at given values of f. The peaks

TABLE 1
λ for H_2^2 and H_2^1 in H_2O Vapor[a]

Frequency (Hz)	λH_2^2	λH_2^1	$\Gamma = \lambda H_2^2/\lambda H_2^1$
0.95	8.89×10^{-4}	4.76×10^{-4}	1.89
3.80	3.51×10^{-3}	1.87×10^{-3}	1.87
11.7	8.90×10^{-3}	4.97×10^{-3}	1.79
23.8	1.12×10^{-2}	7.10×10^{-3}	1.57
34.3	1.03×10^{-2}	7.41×10^{-3}	1.39
100.0	5.71×10^{-3}	5.21×10^{-3}	1.10

[a] The radius $a = 0.19$ cm.

for H_2^2 and H_2^1 are not identical and do not occur at the same value of f. The highest ratio $\Gamma = \lambda_{H_2^2}/\lambda_{H_2^1}$ occurs when $f < 1.0$ Hz. Since best separation occurs when Γ is high and since the yield is likely to be highest at the highest absolute value of $\lambda_{H_2^2}$, one preferably chooses a frequency which promises best separation as well as high yield. We choose for this analysis $f = 11.7$ Hz for a $\Gamma = 1.79$; $D_{\text{eff}L}$ is then 197 cm^2/s, where L stands for the lighter molecule H_2^1.

STEADY-STATE LINEAR GRADIENT BETWEEN TWO RESERVOIRS

The imaginary boundaries of the theoretical model (Appendix) are replaced in a practical application by two reservoirs, (1) and (2), which are connected by capillaries, the radii of which are chosen to provide optimal conditions. For the separation of H_2^2 and H_2^1, radii of 0.2 cm are adequate. The setup is shown schematically in Fig. 1. Reservoir (1) is flushed with a mix of H_2^2 and H_2^1, reservoir (2) with an appropriate carrier fluid, e.g., H_2O vapor. This establishes a constant concentration gradient. A small, reciprocating pump is attached to reservoir (2); it generates the required oscillatory movement of the gas in the capillaries at an angular velocity ω and with an amplitude Δx. The mass transport $\dot{q}$ from (1) and (2) is

$$\dot{q}_i = (c_{i1} - c_{i2}) D_{\text{eff}i} A/L \tag{2}$$

where i stands either for the heavier gas H or the lighter one L, c_1 is the concentration in (1), c_2 is the concentration in (2), and L is the length of the capillaries. For simplicity we define

$$G_i = \frac{\dot{q}_i}{c_{i1} - c_{i2}} = D_{\text{eff}i} A/L \tag{3}$$

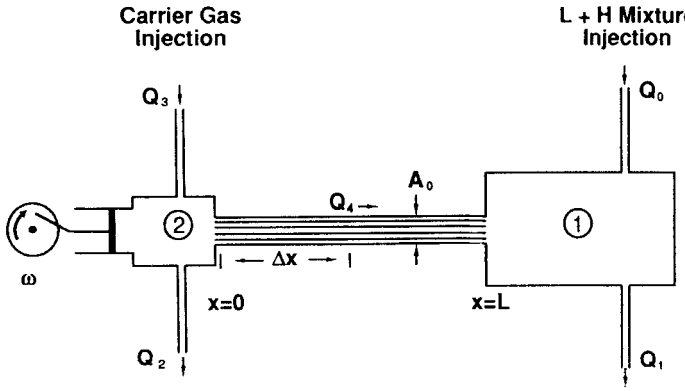

FIG. 1 Schematic of the setup. Two reservoirs, (1) and (2), are connected by capillaries. Reservoir (1) is flushed at a rate of Q_0 with feed, reservoir (2) is flushed at a rate of Q_3 with carrier fluid. A reciprocating pump oscillates the gas in the capillaries with an amplitude Δx. In some experiments a continuous current Q_4 directed against the concentration gradient of the feed is generated.

Using data from Table 1 and a geometry described in more detail below, we find $G_L = 834$ mL/min and $G_H = 1490$ mL/min. The unit mL/min (instead of mL/s) is used for convenience. When container (1) is perfused with a mix of H_2^2 and H_2^1 and container (2) with carrier, a steady state is established with $\dot{q}_H > \dot{q}_L$ since $\lambda_H > \lambda_L$. As a result, the outflow of (2) is enriched in H_2^2 while the outflow of (1) is enriched in H_2^1. Applying the principle of mass concentration, we also have $\dot{q}_i = c_{i2}Q_2$ and $c_{i0}Q_0 = c_{i1}Q_1 + c_{i2}Q_2$. This leads to the following definitions of the transfer fraction f and of the separation ratio s:

$$f_{i2} = \frac{1}{Q_1\left(\frac{1}{Q_1} + \frac{1}{Q_1} + \frac{1}{G_i}\right)} = \frac{c_{i2}Q_2}{c_{i0}Q_0} \tag{4}$$

$$s_{H2} = \frac{\frac{1}{Q_1} + \frac{1}{Q_2} + \frac{1}{G_H}}{\frac{1}{Q_1} + \frac{1}{Q_2} + \frac{1}{G_L}} = \frac{c_{H2}c_{L0}}{c_{L2}c_{H0}} \tag{5}$$

where c_{i2} is, as before, the concentration of H_2^2 or H_2^1 in the inflow of container (2). Note that s_{H2} approaches Γ when Q_1 and Q_2 are large, since $G_H/G_L = \Gamma$; s_{H2}, however, is much reduced if the rates of flushing of the

two reservoirs is low. Note also that Q_1 has to be equal to Q_0 and Q_2 to Q_3 in order to avoid any convective transport of H_2^2 and H_2^1 in the capillaries.

LOGARITHMIC CONCENTRATION GRADIENT BETWEEN TWO RESERVOIRS

Equations (2) and (3) imply a linear concentration gradient along the diffusing path. The gradient between (1) and (2), however, becomes logarithmic if the diffusion takes place in a steady, convective current of the carrier from (2) to (1). This is based on an integration of the Fickian equation first presented by Hertz (7). Hertz observed that, if diffusion takes place against a "counterflow," the diffusion process becomes balanced by the convective current and no net transfer takes place. A logarithmic gradient is established with the tracer concentration falling with distance L from the source:

$$\ln\left(\frac{c_1}{c_2}\right)_i = \frac{Q_4 L}{A D_{mi}} \tag{6}$$

where Q_4 is the rate of the counterflow. Hertz noted that the logarithmic relationship predicts a high separation. The yield, however, is zero!

We generate a counterflow in the setup shown in Fig. 1 by raising Q_3 over Q_2 and Q_1 over Q_0 so that $Q_3 - Q_2 = Q_4 = Q_1 - Q_0$. A new solution of the Fickian equation is derived in which the mass transfer is not completely blocked. A net transport of $\dot{q}_i$ is maintained even though the flux is reduced because of the counterflow. Integration of the Fickian equation gives (8):

$$c_{L1} = c_{L2}e^P + \left(\frac{\dot{q}_L}{Q_4}\right)(1 - e^P) \tag{7a}$$

and

$$c_{H1} = c_{H2}e^{P/\Gamma} + \left(\frac{\dot{q}_H}{Q_4}\right)(1 - e^{P/\Gamma}) \tag{7b}$$

where $P = Q_4/G_L$ is the standardized, nondimensional rate of counterflow. L and H stand for the lighter and the heavier gas, as before. We derive using again the mass conservation principle:

$$f_{H2} = \frac{1}{Q_1\left[\left(\frac{1}{Q_2} + \frac{1}{Q_4}\right)(e^{P/\Gamma} - 1) + \frac{1}{Q_2}\right] + 1} \tag{8}$$

and

$$s_{H2} = \frac{Q_1\left[\left(\frac{1}{Q_2} + \frac{1}{Q_4}\right)(e^{P/\Gamma} - 1) + \frac{1}{Q_2}\right] + 1}{Q_1\left[\left(\frac{1}{Q_2} + \frac{1}{Q_4}\right)(e^{P} - 1) + \frac{1}{Q_2}\right] + 1} \tag{9}$$

Note that $Q_1 = Q_0 + Q_4$ and $Q_3 = Q_2 + Q_4$.

Inspection shows that f and s are dependent on the rates of perfusion Q_0 and Q_3 of the two reservoirs and, more importantly, on the rate of counterflow Q_4 which appears in the exponent P. A very high separation is expected when the rate of counterflow is high; however, the yield falls. This is illustrated in Fig. 2 (line labeled "without") which relates the yield

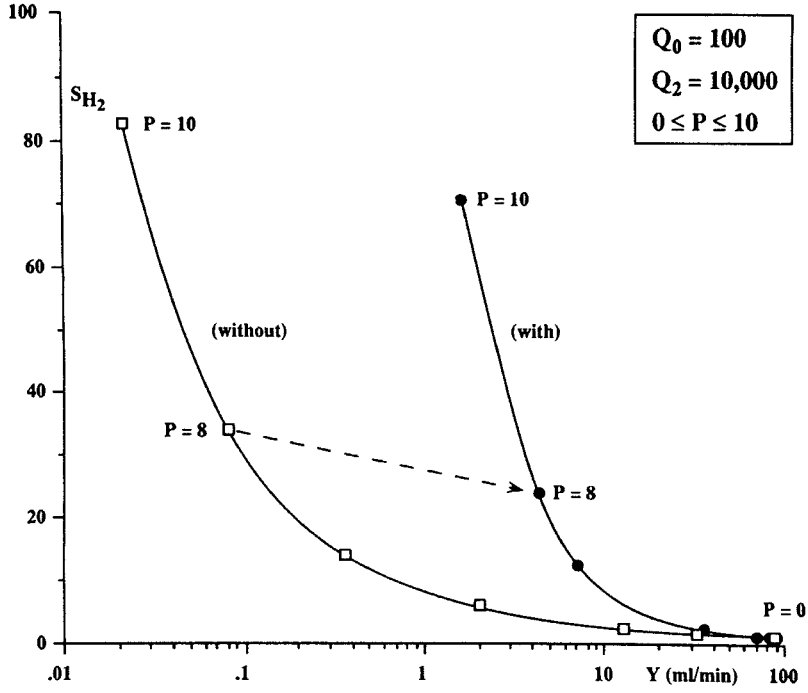

FIG. 2 The separation ratio s_{H2} is plotted against the yield as measured at the exit of reservoir (2) for different values of P; Q_0 and Q_2 are constant. The left-hand curve is obtained without absorber, the right-hand curve with absorber. At given values of P, Q_0, and Q_2, the absorber results in an appreciable increase of yield and a small drop of separation. The small fall of s_{H2} can, of course, be corrected by raising P.

$Y = (\dot{q}_L + \dot{q}_H)$ on the x-axis to the separation on the y-axis. When, e.g., counterflow is raised from zero to $P = 8$, the separation, rises 50-fold; however, the yield falls from 89 to 0.09 mL/min. Figure 2 also shows a second relationship with higher yield (labeled "with") which is discussed in the next section.

IMPROVEMENT OF THE YIELD

The main drawback of using counterflow is the reduction of the diffusional flux. In the following, we propose to make up for some of this reduction.

A closer analysis of the processes involved in counterflow shows that the drop of the flux is due to two mechanisms. The first is related to the altered diffusion process as exemplified by a new Fickian equation (Eq. 7 vs Eq. 2). The second is due to the influx of carrier at a rate of Q_4 into reservoir (1); this influx reduces the concentrations of H and L in that reservoir and the fluxes $\dot{q}_i$ fall proportionately to the drop of c_{H1} and c_{L1}. While the reduction of flux due to diffusion in counterflow is unavoidable, the second can be controlled. We raise c_{H1} and c_{L1} by removing the carrier in reservoir (1). Technical aspects of this procedure are discussed below. Its effect can be evaluated with Eqs. (8) and (9). If the carrier that flows into reservoir (1) as Q_4 is removed by condensation or absorption, the outflow Q_1 falls from a value of $Q_0 + Q_4$ to a value close to or identical with Q_0. The predicted yield $\dot{q}_H + \dot{q}_L$ in the above example rises from

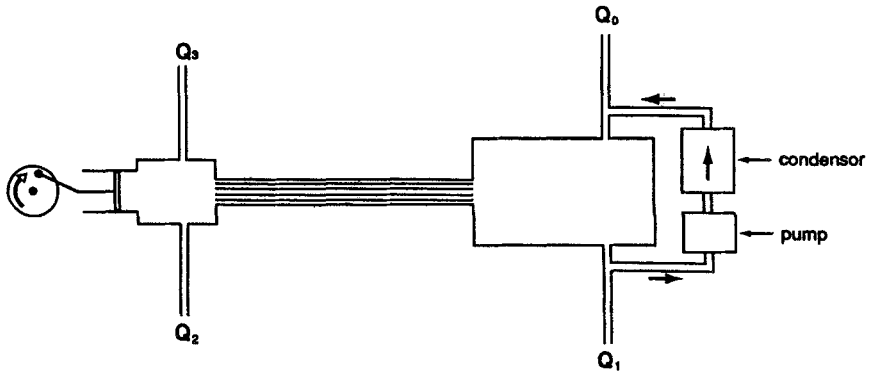

FIG. 3 A condenser is attached to reservoir (1) to remove carrier gas in that reservoir. A pump circulates gas through the condenser. The gas at the exit of the condenser is carrier-free and is reinjected into the reservoir.

the value of 0.09 to 4.35 mL/min; the parameters of the computation are given in the legend of Fig. 2 which illustrates the effect of carrier removal on separation ratio and yield in a more general fashion. The curve marked "with" denotes use of the condenser (as in Fig. 3), and the curve marked "without" has no condenser.

EXPERIMENTAL CONFIRMATION

The laboratory setup is very similar to the schematic given in Fig. 1. Specifically, each reservoir has a volume of 1500 cm^3. Reservoir (1) has a flexible membrane on the side opposite to the capillary entrance. Reservoir (2) is connected to a reciprocating pump that delivers strokes of adjustable volume and frequency. We use a linear pump driven by an sine wave generator and a power amplifier. The pump is separated from reservoir (2) by a second membrane (not shown) to secure airtightness of the system since the reciprocating pump is not perfectly airtight. The capillary bundle consists of 76 capillaries with radius $a = 0.19$ cm and $L = 120$ cm. The tidal volume of gas moving through the capillaries is slightly smaller than the pump's stroke volume because of compression and expansion of gas in reservoir (2). It is measured at an operating frequency with a high speed volume transducer at exit (1) of the capillaries. The oscillation amplitude Δx is defined as the tidal volume/total capillary cross-section area A.

The experiment is run with He and O_2 as diffusing gases and CO_2 as the carrier. The choice of these gases is given by availability of equipment in the author's laboratory. A mix of He and O_2 is injected through a flowmeter into reservoir (1); carrier is injected through another flowmeter into reservoir (2). The outflow of (2) is controlled with a pump and then injected through a CO_2 absorber into three devices which determine the volumetric concentrations of He, O_2, and N_2. The N_2 measurement is used to check for possible leaks that would allow air to enter the system. Another pump controls the outflow of reservoir (1). The four flowmeters for Q_0, Q_1, Q_2, and Q_3 are all calibrated at running conditions with the actual gas mixtures, using a precision wet volumetric flowmeter.

Another pump (Fig. 3) withdraws gas from reservoir (1) and injects it at an adjustable rate into a large CO_2-absorber. The outflow of the absorber reenters reservoir (1). The rate of gas mix pumped through the absorber determines the amount of CO_2 absorbed. This rate is set so that $Q_1 = Q_0$, i.e., CO_2 is absorbed at a rate equal to Q_4.

The molecular diffusion coefficients of He and O_2 in the CO_2 are 0.631 and 0.163 cm^2/s, respectively. The kinematic viscosity of CO_2 is 0.09 cm^2/s. The Schmidt numbers are therefore 0.143 and 0.552, for He and O_2,

TABLE 2
Seven Experimental and Theoretical Values of D_{eff} for the Dispersion of O_2 in CO_2 at Various Frequencies

Testing frequency f (s^{-1})	D_{eff} (exp)	D_{eff} (theory)	Error (%)
1.0	8.74	11.33	−23
1.0	8.74	11.33	−23
2.5	64.25	68.48	−6.2
5	267.20	251.36	+6.3
5	263.20	251.36	+6.3
10	957.93	875.83	+9.4
10	882.68	875.83	+0.8

respectively. The experiment is run at a frequency of 5 Hz which yields a Wormersley number of 3.54 (for definition see Appendix). At these conditions, $\lambda_{O2} = 0.01288$ and $\lambda_{He} = 0.00398$ with a ratio $\Gamma = 3.24$.

A number of experiments were performed with this setup. In a first series, the values of D_{effHe} and D_{effO2} were determined according to the definition of Eq. (3) with $Q_0 = Q_1 = 520$ mL/min and $Q_2 = Q_3 = 520$ mL/min. The experimentally obtained values varied by about 6% from the expected theoretical value (Table 2); two values obtained at 1 Hz had, however, a higher error margin because of the increased technical difficulty to measure very small diffusional fluxes. Note that D_{eff} is highly dependent on frequency. The measured separation ratio s_{H2} was 1.52 ± 0.05; the theoretical value is 1.50. Earlier experiments with a slightly dif-

TABLE 3
Measurement of s_{H2} and Y with Counterflow and Absorption of the Carrier in Reservoir (1)[a]

P	s_{H2} (measured)	s_{H2} (expected)	Y/Q_0
3.5	8.3	10.2	.075
3.6	10.4	10.9	.073
3.7	11.8	11.7	.071
4.7	28.7	23.3	.054
5.3	28.3	35.6	.043
5.3	24.8	35.6	.043
5.3	34.6	35.6	.046
5.3	34.7	35.6	.046

[a] $Y = \dot{q}_{O2} + \dot{q}_{He}$; values of Q_0 and Q_2 varied.

ferent setup gave a similar good agreement between theory and experiment (8).

The second series of experiments included various levels of counterflow. These experimental results are not given for brevity; they confirmed a previously found agreement with the theory (8).

The third series combined counterflow with the use of the absorber attached to reservoir (1). As shown in Table 3, the measured separation came close to the theoretically predicted value; it reached a value (35.6) that exceeds 10 times the ratio of the square root of the molecular weights of the two gases considered, O_2 and He. The yield was about 10% of the input. Without the absorber in reservoir (1), the yield was only 3%. It was not possible to raise the rate of counterflow above $P = 5.3$ because of limits in the capacity of the absorber.

DISCUSSION

The theory of enhanced diffusion describes how gas molecules of different sizes and weights are transported by dispersion in an oscillating carrier; somewhat surprisingly, large gas molecules with a small molecular diffusion coefficient are transported at a higher rate than small molecules with a higher coefficient. The difference is the basis for the proposed separation process. Optimal separation and optimal rate of transport are obtained by tuning the oscillation frequency and the pipe geometry to the gas properties. We make use of the fact that the Fickian equation applies and integrate the equation for a condition in which a constant upstream current of the carrier is superimposed upon the reciprocating oscillatory motion. The counterflow turns the linear concentration gradient of steady-state diffusion between two fixed boundaries into a logarithmic one and separation rises exponentially. The disadvantage of a low yield is met by concentrating the gases in reservoir (1).

The application of the theory to conditions in a bench model raises a number of concerns since we relax some of the assumptions made in developing the theory (4). The main concerns are:

1. The steady upstream current of the carrier distorts the cyclic velocity profiles of the oscillations. No theoretical evaluation of how this distortion affects the transport has been made. However, we assume that the distortion is minimal since the velocity of the counterflow is only about 1/250 of the mean-root-square velocity of the oscillations.
2. The theory is based on the assumption that the diffusing species is highly diluted throughout the length of the diffusing path. We feed, however, an undiluted mix of H and L into reservoir (1). This results

in complex variations of the kinematic viscosity along the diffusing path. The theory, by contrast, assumes that gas properties vary neither with time nor with location. The theoretical evaluation of how this affects the transport has not been completed. It is likely, however, that variations of the kinematic viscosity along the capillaries affect both diffusing gases in a similar fashion so that the separation is not altered.

3. The theory assumes incompressible flow. Working with gases results in compression effects which take place along the diffusing path and in the reservoirs. The pressure drop along the capillaries is about ± 0.01 ata. This allows us, presumably, to assume that gas flow in our experiments is quasi-incompressible.
4. There are, presumably, entrance effects at each capillary end. The velocity profiles in those sections are not fully understood since a theory of entrance effects in oscillatory flows is not yet available. End effects have been studied in the special case of porous membranes, however (9).
5. The two reservoirs have to be perfectly mixed in order to conform with the boundary conditions of the theory; in theory, the concentration in the reservoirs has to be constant at all times throughout the containers. Specifically, the application of the theory to the bench model implies that the concentration gradient is the same for each of the 76 capillaries and that the exit concentrations c_{H2} and c_{L2} are the same as the concentrations at the capillaries as they open into reservoir (2). We have confirmed experimentally that the mixing in both reservoirs is excellent, presumably because of the effects of cyclic jet formation. However, the available measuring devices do not match the stringent requirements of the theory; specifically, we are not able to investigate the time course of the concentration in the vicinity of the capillary openings in the two reservoirs.

The above concerns are alleviated in part by the good agreement of experimental results with the theory. The agreement holds true for three experimental configurations, namely transfer without counterflow, with counterflow, and when the counterflowing carrier is also absorbed in reservoir (1). These agreements suggest that the experimental setup is adequate in meeting the stringent assumptions of the theory.

There were limitations set by the experimental apparatus used. Thus, the equipment had a resolution that limited measurements of gas concentrations to values exceeding 1–2%. Moreover, the CO_2 absorber had a capacity that limited experiments to a rate of counterflow not exceeding $P = 5.3$ or 1500 mL CO_2/min. We believe that with better equipment, e.g.,

by condensing rather than absorbing the carrier gas, much higher rates of counterflow could be handled.

An attractive feature of the method is its adaptability. The separation ratio may be varied by about two orders by merely adjusting the rate of counterflow. The yield changes inversely, but removal of the carrier by condensation in reservoir (1) reduces the loss of yield. Thus, the separation ratio was raised in our experiments from 1.50 to 35.6 while the yield fell only from 115 to 24 mL/min. The theory predicts even better results at higher rates of counterflow. As mentioned earlier, we were not able to perform experiments at such high rates of counterflow.

The ease of adjusting the separation ratio and yield is useful in designing cascades for a prescribed enrichment task. Such cascades typically require a high yield in the early stages and a high separation ratio in the latter stages. This is achieved by varying the rate of counterflow. We illustrate this with an example using the enrichment of deuterium. Let us assume that H_2^2 is to be enriched 1000:1. Let us assume further the availability of equipment similar to that used in our laboratory experiments but adapted for the separation of H_2 isotopes with water vapor as the carrier. The performance of such a system is predicted by using the values of λ listed earlier. Table 4 lists some relevant results; it is seen that the 1000:1 purification is achieved in three stages. The first two stages are run at a low rate of counterflow. The first stage has a total cross-sectional area 10 times larger than our laboratory unit; the third stage has the same geometry as the laboratory system. The yield of the cascade is 2.24 mL/min or 0.01% of the original feed. If one assumes that the operation cost is mostly due to the need to recycle water vapor, one may make the following cost estimate: the production of 2.24 mL/min of enriched material requires 221 L/min of carrier and a power consumption of about 0.66

TABLE 4
Three-Stage Cascade for the H_2^2 Purification[a]

Stage	P	Q_0 (mL/min)	Q_2 (mL/min)	s	Size	Yield (mL/min)
1	4	2000	10,000	5.6	10:1	450.0
2	5	450	10,000	6.96	5:0	100.0
3	8.2	100	10,000	26.75	1:1	2.24
				1043		

[a] Summary: Total purification: 1043:1; final yield: 2.24 mL/min. Total need for carrier (Q_3 times size of stage): 221 L/min.

kW. The energy cost of 1 L of product is 5 kWh. This estimate does not account for energy savings by recovering some of the cooling energy. Such standard procedure would reduce the energy cost very appreciably, especially in large-scale operations.

It is difficult to compare the proposed method with other methods used presently to enrich isotopes of hydrogen since the method is in its infancy. Consideration should be given to its potential rather than to the achievement. Little or no work has been done to try to test possible improvements such as increasing Δx (Eq. 1) or increasing the operating pressure to increase molar yield. A promising prediction based on the above theory shows that the energy cost in kW/L yield rises quasi-linearly with the separation ratio. One might have expected a relationship in which the cost skyrockets when higher separation is demanded.

Another interesting aspect is given by the possibility of combining the proposed separation process with fractional distillation, which is one of the major methods presently used to enrich heavy water. The recycling of the carrier mentioned earlier as the main energy-requiring process in the present system is in fact identical with fractional distillation and could therefore be combined with fractional distillation to further reduce operating costs.

APPENDIX: MECHANISM OF DISPERSION IN OSCILLATORY FLOWS

The phenomenon of transport enhancement of contaminants was initially investigated by Taylor (1) and Aris (10) in their studies of axial dispersion in steady flows within capillary tubes. Their results indicated that a significant increase in axial contaminant dispersion will occur in steady laminar flows. Similar effects were found to exist for oscillating flows by Dreyer (3). Harris and Goren (11) studied, both analytically and experimentally, the mass transfer through a long tube connecting two containers by oscillating the flow in the tube and found an increase of mass transfer between two containers by orders of magnitude. Kurzweg and Jaeger (12) first showed the existence of a "tuning" characteristic of mass diffusion by oscillating flows and suggested its use for gas separation. The proposed separation is based on this tuning effect which is explained in detail below.

Assume that a long cylindrical pipe filled with two different gases is set up horizontally. On the right is pure N_2, on the left a mixture of O_2 and N_2 in the proportion 10/90, respectively. At the beginning the interface between the two gases is a vertical plane with the surface area of the cross-section, as shown in Fig. 4(a). The transport of O_2 from left to right

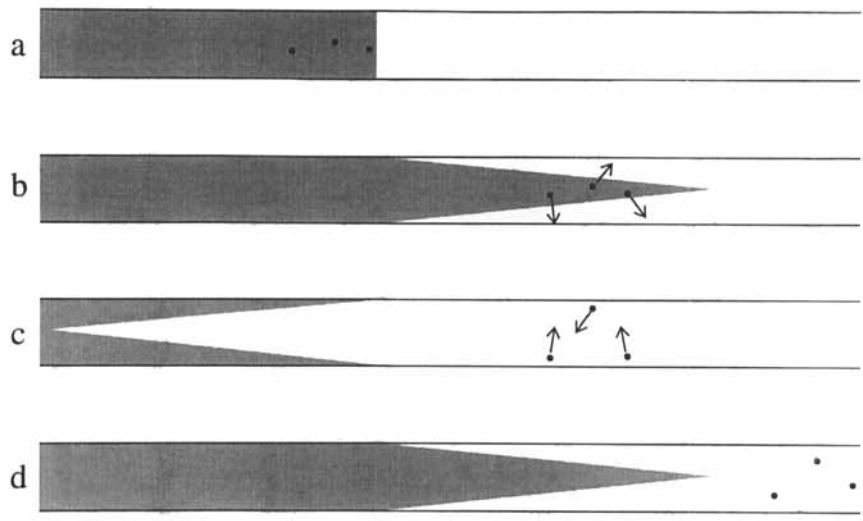

FIG. 4 Schematic diagram of the mechanism of enhanced diffusion. Discussed in detail in the Appendix.

is characterized by its molecular diffusion coefficient D_m through Fick's law.

If a time-periodic hydrostatic pressure gradient is applied to the gases, an oscillatory flow will be established. The flow and the associated concentration distribution will reach a "steady time-periodic" state several cycles after the oscillation starts. Here, the phrase "steady time-periodic" means that the flow and concentration fields are still a function of time, but they repeat periodically without any change between every pair of cycles. Now, let us look at the mass transport at a given point in the pipe.

During the part of the oscillation cycle when the flow is from left to right, a spike occurs because of viscous shear. This forces the fluid particles near the pipe wall to remain at rest. As a result, the interface between the O_2/N_2 gas mixture and the pure N_2 is elongated and its surface area is enlarged. Diffusion of O_2 now occurs not only in the axial direction but, more importantly, also in the radial direction from the core into the boundary layer as illustrated by the arrows in Fig. 4(b). This radial diffusion is promoted both by the interface area being larger than the cross-section of the pipe and also by a concentration gradient between the core and the region close to the pipe wall which is much greater than the initial axial concentration gradient. A certain amount of O_2 is transported from the core to the boundary layer through this radial diffusion. At the moment the convective flow

is reversed, the diffusion situation is also reversed since the radial concentration gradient changes its direction. The molecules that have just diffused radially will diffuse back into the center of the pipe where the fluid with low O_2 concentration comes from the right-hand side. This is illustrated in Fig. 4(c). When the flow comes again from the left, the core-to-wall diffusion also comes, but with fresh O_2 molecules from the left-hand side of our viewing point. The O_2 molecules that were at our viewing point have moved to the right-hand side by the flow, as shown in Fig. 4(d), and diffuse to the boundary layer there. As the flow goes back and forth, the above core-to-wall-to-core procedure will repeat itself again and again. The O_2 molecules, then, will be transported from the left to the right with many steps of stopping at the boundary layer and reboarding on the core flow. This transforms the axially reciprocating, convectional motion into a unidirectional mass transfer of O_2 from left to right.

It may be intuitively clear that timing plays a key role in optimizing the dispersion in oscillatory flows. The time periods allowed for the two processes, the axial convective motion of the fluid and the radial diffusion of the molecules, have to match each other for an optimization of time-averaged unidirectional mass transfer. If the axial motion is so fast that the radial diffusion can not be completed in the time period provided to it, the net amount of O_2 transported axially will be very little since only a few molecules are able to diffuse between boundary layer and core region. On the other hand, a small overall axial mass transfer will occur when the axial motion is too slow compared with the radial diffusion speed, because the O_2 molecules have to stay at the boundary layer, or the core region, for a longer time waiting for the large radial concentration gradient established by the axial convective flow. The maximum mass transfer occurs when the diffusion time from pipe axis to its wall is approximately equal to half of the oscillation period and which we call the "tuning" condition in our discussion.

From primary principles, Kurzweg (5) derived the following generalized equation to describe the effective diffusion coefficient:

$$D_{\text{eff}} = \lambda \omega \Delta x^2$$

where ω is the angular frequency of the flow oscillation and Δx is the oscillation amplitude. The nondimensional factor λ depends on the radius of the pipe, the kinematic viscosity of the gases, the molecular diffusion coefficient D_m, and the oscillation frequency. In mathematical expression, they are grouped to two dimensionless number: The Womersley number $\alpha = a\sqrt{\omega/\upsilon}$ and the Schmidt number $\sigma = \nu/D_m$, where a is the radius of the pipe and υ is the kinematic viscosity of the gases. The dependence of λ on these parameters can be expressed in a set of equations.

TABLE A1

Gas $0.1 < \sigma < 2.0$	$\alpha < 1$ $\lambda = \sigma\alpha^2/384$	$\alpha > 20$ $\lambda \approx 1/12\sqrt{2\alpha}$
Liquid $500 < \sigma < 5000$	$\alpha < 0.01$ $\lambda = \sigma\alpha^2/384$	$\alpha > 1$ $\lambda \approx 1/4\sqrt{2\sigma\alpha}$

$$\lambda(\alpha,\sigma) = D_{\text{eff}}/\omega X^2 = AB/C$$

with

$$A = \sigma/4\alpha(\sigma^2 - 1)$$

$$B = F_1(\alpha) - \frac{1}{\sqrt{\sigma}}\left[\frac{|F(\alpha)|}{|F(\alpha\sqrt{\sigma})|}\right]^2 F_1(\alpha\sqrt{\sigma}); \qquad F(\alpha) = F_R(\alpha) + iF_1(\alpha)$$

$$C = |1 + 2F(\alpha)/\alpha|^2$$

$$F_R(\alpha) = [\text{bei } \alpha \text{ ber}' \alpha - \text{ber } \alpha \text{ bei}' \alpha]/[\text{ber}^2 \alpha + \text{bei}^2 \alpha]$$

$$F_1(\alpha) = [\text{ber } \alpha \text{ ber}' \alpha + \text{bei } \alpha \text{ bei}' \alpha]/[\text{ber}^2 \alpha + \text{bei}^2 \alpha]$$

The relationship $\lambda(\alpha,\sigma)$ simplifies for a number of boundary conditions given in Table A1.

ACKNOWLEDGMENT

The author acknowledges the editorial help of Dr. A. Zhao, Department of Chemical Engineering, University of Florida, who wrote the short description of the mechanism in the Appendix.

GLOSSARY

a	radius of pipe (cm)
A	total cross-sectional area of all capillaries (cm^2)
c	volumetric concentration (mL/mL)
D_{eff}	effective diffusion coefficient (cm^2/s)
D_m	molecular diffusion coefficient (cm^2/s)
f	transfer fraction (—)
G	diffusional conduction defined Eq. (3) (mL/min)
H	heavy diffusing species (—)
L	light diffusing species (—)

L length of capillary (cm)
P standardized counterflow (—)
$\dot{q}$ diffusional flux of either L or H (mL/min)
Q convectional flows in and out of reservoirs (mL/min)
Δx average oscillation amplitude (cm)
s separation ratio (—)
Γ $D_{\text{effH}}/D_{\text{effL}}$ (—)
λ standardized effective diffusion $D_{\text{eff}}/\omega\Delta x^2$ (—)
ν kinematic viscosity of carrier (cm^2/s)
ω angular velocity (r/s)

REFERENCES

1. G. Taylor, *Proc. R. Soc., Ser. A, 219*, 186–203 (1953); *223*, 446–468 (1954).
2. P. C. Chatwin, *J. Fluid Mech., 71*, 513 (1975).
3. G. Dreyer et al., *Z. Naturforsch., 23*, 498 (1967).
4. E. J. Watson, *J. Fluid Mech., 133*, 233–244 (1983).
5. U. Kurzweg and M. Jaeger, *Phys. Fluids, 29*, 1324 (1986).
6. M. Jaeger, T. Soepardi, and A. Maddahian, *Sep. Sci. Technol., 26*, 503–514 (1991).
7. G. Hertz, *Z. Phys., 91*, 810 (1923).
8. M. Jaeger, P. Kalle, and U. Kurzweg, *Sep. Sci. Technol., 27*, 691–702 (1992).
9. A. K. Chandhok and D. Leighton, *Chem. Eng. Sci., 46*, 2661–2668 (1991).
10. R. Aris, *Proc. R. Soc., Ser. A, 235*, 67–77 (1956).
11. H. G. Harris and S. L. Goren, *Eng. Sci., 22*, 1571 (1967).
12. U. Kurzweg and M. Jaeger, *Phys. Fluids, 30*, 1023–1025 (1987).

Received by editor July 17, 1995